

Published in final edited form as:

Brain Res. 2011 March 10; 1378: 54–65. doi:10.1016/j.brainres.2011.01.028.

Olivary Climbing Fiber Alterations in PN40 Rat Cerebellum Following Postnatal Ethanol Exposure

Dwight R. Pierce^{a, *}, Abdallah Hayar^b, D. Keith Williams^c, and Kim Edward Light^a

^aDepartment of Pharmaceutical Sciences University of Arkansas for Medical Sciences 4301 W. Markham St., #522-3 Little Rock, Arkansas 72205-7199 USA lightkime@uams.edu

^bDepartment of Neurobiology and Developmental Sciences University of Arkansas for Medical Sciences 4301 W. Markham St., #847 Little Rock, Arkansas 72205-7199 USA AMHayar@uams.edu

^cDepartment of Biostatistics University of Arkansas for Medical Sciences 4301 W. Markham St., #781 Little Rock, Arkansas 72205-7199 USA WilliamsDavidK@uams.edu

Abstract

Developmental ethanol exposure in rats during postnatal days (PN) 4–6 is known to cause significant loss of cerebellar Purkinje cells. It is not known what happens to the surviving neurons as they continue to develop. This study was designed to quantify the interactions between the olivary climbing fibers and the Purkinje cells when the cerebellar circuits have matured. Rat pups were treated with a daily dose of ethanol (4.5 g/kg body weight) delivered by intragastric intubation on PN4, PN4–6, or PN7–9. The interactions between climbing fibers and Purkinje cells were examined on PN40 using confocal microscopy. Mid-vermal cerebellar sections were stained with antibodies to calbindin-D28k (to visualize Purkinje cells) and vesicular glutamate transporter 2 (VGluT2, to visualize climbing fibers). Confocal z-stack images were obtained from Lobule 1 and analyzed with Imaris software to quantify the staining of the two antibodies. The VGluT2 immunostaining was significantly reduced and this was associated with alterations in the synaptic integrity, and synaptic number per Purkinje cell with only a single exposure on PN4 enough to cause the alterations. Previously, we demonstrated similar deficits in climbing fiber innervation when analyzed on PN14 (Pierce, Hayar, Williams, and Light, 2010). The present study confirms that these alterations are sustained and further identifies the decreased synaptic density as well as alterations to the general morphology of the molecular layer of the cerebellar cortex that are the result of the binge ethanol exposure.

Keywords

Purkinje cell; Climbing fibers; Imaris; Confocal; VGluT2; Development

© 2011 Elsevier B.V. All rights reserved

*Dwight R. Pierce (corresponding author) piercedwight@uams.edu Phone: (501)686-5542 Fax: (501)686-6057.

Publisher's Disclaimer: This is a PDF file of an unedited manuscript that has been accepted for publication. As a service to our customers we are providing this early version of the manuscript. The manuscript will undergo copyediting, typesetting, and review of the resulting proof before it is published in its final citable form. Please note that during the production process errors may be discovered which could affect the content, and all legal disclaimers that apply to the journal pertain.

1. Introduction

The cerebellum is vulnerable to developmental ethanol exposure, and in the rat, exposure on postnatal days (PN) 4–6 targets survival of the cerebellar Purkinje cells (PCs) as well as the early distribution of olivary climbing fibers (Goodlett et al., 1990, Goodlett and Lundahl, 1996, Pierce et al., 1999, Dikranian et al., 2005, Pierce et al., 2010). The magnitude of Purkinje neuron loss is directly proportional to the blood ethanol concentration achieved when exposure lies within this vulnerable period (Bonthius and West, 1990, Goodlett et al., 1990, Goodlett et al., 1997, Pierce et al., 1999). The inferior olivary neurons are also vulnerable to ethanol during this period and reductions of as much as 25% are reported after ethanol exposure during this time frame (Napper and West, 1995, Dikranian et al., 2005). The rat brain development during the first week of postnatal life is a period of rapid growth similar to that found for human brain development during the early weeks of the third trimester (Dobbing and Sands, 1979, Dobbing, 1981, Cudd, 2005). Administering a high dose of ethanol to rat pups each day for the three day vulnerable period (PN4-6) is a well established model that mimics binge drinking during the human third trimester equivalent period (Hamre and West, 1993, Goodlett and Lundahl, 1996, Pierce et al., 1999, Dikranian et al., 2005, Pierce et al., 2010).

Binge drinking (five or more drinks at the same time or within a couple of hours) occurs in 32.6% of non-pregnant women (NSDUH, 2009). Studies of pregnant women report a that only 1% of pregnant women engage in binge drinking during their third trimester of pregnancy (NSDUH, 2009). Nevertheless, this 1% accounts for 40,000 to 60,000 children per year in the USA (NSDUH, 2009, Ventura et al., 2008). Interestingly, this rate for binge drinking during the third trimester is coincident with the estimated incidence rate for Fetal Alcohol Spectrum Disorder (FASD) of 1 in every 100 live births (Riley and McGee, 2005, 2009).

Previously, we reported that the cerebellar cortex of PN14 rat pups exposed to binge ethanol during PN4-6 showed significant alterations in the inferior olivary input. The number of Purkinje cells was decreased as previously reported, but additional alterations were identified that involve the development of the surviving Purkinje neurons and their receipt of significantly fewer climbing fiber inputs beyond what would be expected by the reduction in cell numbers (Pierce et al., 2010). This present study follows the same approach to identify the answer to several questions. Are the alterations in climbing fiber input identified at PN14 sustained? Does the analysis of co-localization of climbing fiber and Purkinje elements provide evidence of decreased synaptic contacts? Finally, is there evidence of delayed developmental damage in the group exposed to ethanol during PN7-9, when a reduction of PCs will not be produced?

Climbing fibers, arising from the contralateral inferior olivary nucleus in the brain stem, represent one of two major extrinsic inputs to the Purkinje cells. The other major input is from the mossy fibers via granule cell axons known as parallel fibers (Altman and Bayer, 1997, Watanabe, 2008). Although the climbing fibers comprise only 1–2% of the synapses on the Purkinje cells, they have a critically important role in the proper functioning of the cerebellar circuitry (Strata and Rossi, 1998, Ito, 2001, Watanabe, 2008). Alterations of climbing fiber development (e.g. glutamate receptor gene deletion) produces significant ataxia, motor discoordination, and disturbances of eye blink conditioning (Ichise et al., 2000, Hashimoto et al., 2001, Kishimoto et al., 2002, Kato et al., 2005). These behavioral deficits are very similar to those documented in rats postnatally exposed to ethanol (Meyer et al., 1990, Thomas et al., 1996, Thomas et al., 1998, Klintsova et al., 2002, Green, 2004) and in human FASD (Streissguth et al., 1980, Roebuck et al., 1998, Coffin et al., 2005, Connor et al., 2006).

We hypothesized that ethanol exposure to the rat on PN4-6 would continue to induce, on PN40, significant alterations in the climbing fiber input to the Purkinje cells in support of a sustained negative impact on cerebellar functioning. In addition, these differences will be consolidated to the cerebellar molecular layer and not the soma, as this region contains much less innervation from climbing fibers when mature. In addition, we hypothesize that analysis of co-localization will show evidence of decreased synaptic contacts from climbing fibers per PC. While we also suspect that the later ethanol exposure period (E7-9) will demonstrate detrimental impact on climbing fiber innervation, we do not expect this to be of great magnitude. To test these hypotheses, climbing fiber synapses were visualized in lobule I of cerebellar sections immunostained for vesicular glutamate transporter 2 (VGluT2) (Hioki et al., 2003, Miyazaki et al., 2003, Takagishi et al., 2007) with Purkinje cell visualization using immunostaining for calbindin-D28k (CalB) (Light et al., 2002). Confocal z-stack images were 3D-reconstructed and quantified as the total expression intensity and the volume of expression in the soma and molecular layers, utilizing Imaris software (Bitplane AG, Zurich, Switzerland) (Hein et al., 2006, Marvizon et al., 2007, Nassimi et al., 2009).

2. Results

2.1 Blood Ethanol Concentration (BEC)

The mean BEC for the ethanol group (4.5 g/kg) was 365.4 ± 38.6 mg/dl (\pm SEM) ($n = 7$) as previously reported (Pierce et al., 2010).

2.2 Body weight data

The body weights of the rats at PN40 were analyzed for each group (Fig. 1). There was a significant interaction ($F_{(2,29)} = 4.3$; $p < 0.05$); however, custom contrasts ($p < 0.05$) did not verify any significant differences. This indicates that the general growth of the rats was not significantly affected by ethanol exposure.

2.3 Cell count data

Figure 2 presents the results from the Purkinje cell counting within lobule I. No significant interaction ($F_{(2,30)} = 1.5$; $p > 0.05$) was identified; however, a significant main effect of treatment ($F_{(1,30)} = 16.3$; $p < 0.01$) and no significant main effect of timing ($F_{(2,30)} = 1.5$; $p > 0.05$) were observed. Thus, postnatal ethanol exposure produced a significant decrease in the number of Purkinje neurons in lobule I of the 40-day old rat as expected. In addition, we observed from the custom contrasts that significant differences were identified for the E4 vs C4 and the E4-6 vs C4-6 comparisons.

These data were obtained from 10 μ m sections of the cerebellar midline and the numbers of animals within each group are slightly different from the numbers involved in the confocal analyses of 60 μ m sections (see Table 1 and Methods).

2.4 Molecular Layer Analyses

Calbindin D28k positive immunofluorescent labeling was used to identify Purkinje cells and concurrent VGluT2 positive immunofluorescent labeling was used to identify climbing fiber innervation of the Purkinje cells in lobule I. VGluT2 immunoreactivity represents the nerve terminals of the climbing fibers from the inferior olivary nucleus. There are two main glutamate transporters in the cerebellar cortex, VGluT1 and VGluT2 (Hioki et al., 2003). Parallel fibers from granule cells in adult animals express VGluT1 (Hioki et al., 2003, Miyazaki et al., 2003). Climbing fiber terminals consistently exhibit VGluT2 immunoreactivity in the molecular layer (MolLay) and in the Purkinje cell soma layer (Hioki et al., 2003, Miyazaki et al., 2003, Takagishi et al., 2007). The immunostaining of

VGluT1 and VGluT2 is localized only to nerve terminals and not to cell bodies or dendrites (Fremeau et al., 2004).

Figure 3 shows the rendered Imaris image with each channel shown independently, (A. CalB, B. VGluT2) and merged (C). The blue line outlines the Soma region to indicate the division of these images into the Soma and the molecular layer (MolLay) regions for analyses.

Within these two specific regions (Soma, MolLay), the analysis of climbing fiber development as measured by VGluT2 immunostaining was determined as the summed intensity or volume of the voxels within the VGluT2 channel in the region. The volume represents the size of the tissue compartment expressing the protein and the intensity was interpreted as a measure of the total expression level of that protein. Since it is known that ethanol exposure results in a decreased number of Purkinje cells, the summed VGluT2 volume or summed VGluT2 intensity of each sample was divided by the total volume of the calbindin-D28k channel (Purkinje cell specific) of that same sample and region in order to normalize the data and obtain the VGluT2 volume or intensity per micron³ of Purkinje cell tissue. Thus any group differences in these values are not the result of the ethanol-induced loss of Purkinje cells. These two end-points were termed **VGluT2 Intensity Ratio**, and **VGluT2 Volume Ratio** (Table 2). The Imaris software also allowed the construction of a channel that includes only those voxels that contained both red and green fluorescence and was termed the co-localized channel. As described above the summed volume or intensity of the co-localized voxels in each region of interest were divided by the total volume of the calbindin-D28k channel in order to normalize these measures to the volume of Purkinje cell tissue. These two end-points were termed **Co-localized Intensity Ratio** and **Co-localized Volume Ratio** (Table 2). We have interpreted the co-localized end-points as representing the portion of the climbing fiber tissue that had made putative functional contacts with Purkinje cells. Each of these four endpoints was determined in the Soma and Molecular Layer regions of each tissue sample independently and in a blind-to-treatment manner.

By PN40, the VGluT2 positive immunofluorescent labeling was represented as distinct puncta in the molecular layer region of lobule I. The number of these puncta was determined using the Imaris program, and the data were normalized by dividing the number of puncta by the number of Purkinje cells in the specific confocal slice (**VGluT2 Puncta/PC**) (Table 2). In addition, the co-localized puncta were also counted and normalized to the number of Purkinje cells in the specific confocal section (**CoL-Puncta/PC**) (Table 2).

Finally, the width (or radial distance) of the molecular layer was measured using the reconstructed images from the confocal image z-stacks obtained from mid-sagittal slices of the lobule I region. Measurements were made of the molecular layer by recording the distance from the edge demarcated between the soma layer and the molecular layer to the pial surface of the molecular layer using only the CalB channel. For each tissue image analyzed, we calculated an average of four of these measurements that were made across the extent of the sample. This **MolLay Width** (Table 2) provided a comparative metric of the developmental extent of the cerebellar cortex.

The results of the analyses of climbing fiber innervation within the MolLay region are presented in Figures 4–6. For climbing fiber innervation to the MolLay region, there was no significant interaction ($F_{(2,29)} < 1$), and no significant main effect of treatment ($F_{(1,29)} < 1$) or timing ($F_{(2,29)} < 1$) of the VGluT2 Intensity Ratio (Fig. 4A). However, the Co-localized Intensity Ratio (Fig. 4B) demonstrated a significant interaction ($F_{(2, 29)} = 5.1$; $p < 0.02$) with custom contrasts at the $p < 0.05$ level identifying significant differences for E4 vs C4 and E4-6 vs C4 -6.

The VGluT2 Volume Ratio within the MolLay region (Fig. 4C) did not show a significant interaction ($F_{(2, 29)} = 1.1$; $p > 0.05$). However, a significant main effect of treatment ($F_{(1, 29)} = 22.9$; $p < 0.01$) with no significant main effect of timing ($F_{(2, 29)} = 2.8$; $p > 0.05$) was observed. Clearly, postnatal ethanol exposure results in a loss of volume for climbing fiber tissue within the cerebellar cortex. The custom contrasts at the $p < 0.05$ level provide further insights as significant differences were identified for the E4 vs C4, E4 vs E7-9, E4-6 vs C4-6, and E4-6 vs E7-9 comparisons.

Finally, the Co-localized Volume Ratios within the MolLay (Fig. 4D) showed a significant interaction ($F_{(2, 29)} = 5.1$; $p < 0.02$). Custom contrasts at the $p < 0.05$ level identified significant differences for E4 vs C4, E4 vs E7-9; E4-6 vs C4-6, E4-6 vs E7-9; and E7-9 vs C7-9. Thus, the impact of ethanol exposure on climbing fiber innervation of the cerebellar cortex is a significant and somewhat profound decrease in both climbing fiber tissue and that portion that is co-localized with the Purkinje cell targets.

Since the VGluT2 positive immunofluorescent labeling at PN40 consists of distinct puncta throughout the MolLay region of lobule I (see Fig. 3B) we counted these puncta and then normalized them to the number of Purkinje cells (PC) within the analyzed slice (Fig. 5). The VGluT2 Puncta/PC (Fig. 5A) showed no significant interaction ($F_{(2, 29)} = 3.2$; $p > 0.05$) and no significant main effect of treatment ($F_{(1, 29)} = 1.9$; $p > 0.05$). However, a significant main effect of timing ($F_{(2, 29)} = 5.4$; $p < 0.02$) was present. This main effect of timing consisted of differences between the 4 and 4–6 groups compared to the 7–9 period. The effect is clarified when the custom contrasts are inspected and reveal significant differences only for E4 vs E7-9, and E4-6 vs E7-9.

Analysis of the Co-localized Puncta /PC (Fig. 5B) values reveals a significant interaction ($F_{(2, 29)} = 3.7$; $p < 0.05$). The custom contrasts identify significant differences for E4 vs C4, E4-6 vs C4-6 and E4-6 vs E7-9.

2.5 Molecular layer width

The apparent width or radial distance of the molecular layer (Fig. 6) did not show a significant interaction ($F_{(2, 29)} = 2.2$; $p > 0.05$). However, significant main effects of both treatment ($F_{(1, 29)} = 6.9$; $p < 0.02$) and timing ($F_{(2, 29)} = 4.9$; $p < 0.02$) were identified. We conducted the custom contrasts at the $p < 0.05$ level in order to obtain further insights and observed significant differences for E4 vs E7-9, E4-6 vs C4-6, and E4-6 vs E7-9.

2.6 Soma Region Analyses

The analysis of these parameters in the Soma region of PN40 rats revealed only a main effect of ethanol to decrease the Co-localized Volume Ratios (Fig. 7C).

3. Discussion

This study confirms that the Purkinje neurons surviving the extensive neuronal death induced by binge-like ethanol exposure during the postnatal vulnerable period of the rat are also damaged in their interaction with the critical input of information delivered by climbing fibers from the inferior olive neurons. Previously we showed significant decreases of climbing fiber innervation at PN14 of the rat brain development (Pierce et al., 2010), and the present study demonstrates that those decreases are sustained, and likely permanent. Our normalization of the climbing fiber measurements to the volume (or number) of Purkinje neurons (that survived ethanol exposure) allows the interpretation that these alterations were not merely reflective of the Purkinje cell loss; rather they demonstrate an altered trajectory of development in the cerebellar cortex.

Two important aspects of climbing fiber innervation of the Purkinje cells were decreased in the E4 or E4-6 groups. The VGluT2 Volume Ratio (Fig. 4) identifies the total volume of tissue expressing VGluT2, and thus climbing fiber innervation (normalized to the total volume of PC tissue). Both E4 and E4-6 treatments resulted in significant decreases in this parameter; however, they were not significantly different from each other. This supports the conclusion that a single binge exposure to ethanol is sufficient to produce the damage identified providing it is delivered during the PN4-6 vulnerable period. We therefore conclude that either fewer climbing fibers are providing the innervation or there is decreased branching of the climbing fibers present. The later seems perhaps more likely in light of the normal condition of one climbing fiber innervating a Purkinje cell. Analysis of the Co-localized Volume Ratio and the Co-localized Intensity Ratio (Fig.4D) demonstrates that the actual magnitude of climbing fiber innervation to the surviving Purkinje cell is decreased with E4 and E4-6 exposures. Assuming that the co-localized endpoints are surrogates of functional contacts between climbing fibers and Purkinje cells then a decrease in the functional interactions between climbing fibers and Purkinje cells is suggested.

Further support for the above findings is seen in the analyses of the number of climbing fiber puncta per Purkinje cell (Fig. 5). Again, the VG2 Puncta/PC shows significant decreases for E4 and E4-6 only when compared to the E7-9 group. However, when analysis is focused on the co-localized puncta (CoL-Puncta/PC, Fig 5B) the E4 treatment resulted in a significant decrease compared to controls and the E4-6 resulted in a significant decrease compared to control and E7-9 (but not E4). Again the conclusion that the surviving Purkinje cells receive fewer climbing fiber synaptic contacts is supported. These findings strongly point to a cerebellar circuit that is likely deficient since climbing fiber innervation, while relatively minor compared to total synaptic innervation of Purkinje neurons, is critical in triggering long-term depression (Carta et al., 2006).

According to the literature, the number of inferior olivary neurons is decreased following E4 or E4-6 ethanol exposure (Napper and West, 1995, Dikranian et al., 2005). The loss of inferior olivary neurons is not trivial, since the climbing fibers are the axons of these neurons. However, it is important to point out that the timing of ethanol exposure in these studies occurs during the creeper stage (PN3-7) of climbing fibers development when the inferior olivary axons have an overabundance of branches. During normal development, a single inferior olivary axon at PN3-7 will have more than 100 climbing fiber branches (Sotelo, 2004, Sugihara, 2006). The climbing fiber innervation to Purkinje neurons during this period is concentrated around the soma and each Purkinje cell may receive input from 14 climbing fiber branches, since the ratio of Purkinje neurons to inferior olivary neurons is 7 to 1 (Mason et al., 1990, Altman and Bayer, 1997, Sugihara, 2005, Sugihara, 2006). With normal development, the overabundance of climbing fibers eventually translocate from the soma to the dendrites of the molecular layer and are reduced to a final state of seven climbing fiber branches per olivary neuron and a single Purkinje cell innervated by a single climbing fiber branch (Altman and Bayer, 1997, Lopez-Bendito et al., 2001, Sotelo, 2004, Sugihara, 2006). Even if postnatal ethanol exposure reduced the number of inferior olivary neurons in a greater proportion than Purkinje cells, there would still be an overabundance of climbing fiber branches to potentially produce the typical development of climbing fiber distribution.

We have also identified evidence of significant remodeling of the molecular layer when a substantial number of the Purkinje cells have been killed. This remodeling appears as a significant reduction of the radial width of the molecular layer (Fig. 6) following E4 and E4-6 treatments. This finding suggests significant remodeling of the developing molecular layer following the loss of more than a third of the Purkinje neurons. The result is a molecular layer that contains the same total volume of Purkinje cell tissue compacted within

a shorter radial width molecular layer suggesting that the dendritic tree of these neurons developed within the space formerly occupied by the now dead Purkinje neurons. Thus, the density of the molecular layer is maintained, while the radial width is reduced.

During normal cerebellar development climbing fibers at PN15 have usually reached the adult configuration with their extensive distribution around the proximal dendrites of the Purkinje cells and minimal soma based contacts (Lopez-Bendito et al., 2001, Sotelo, 2004, Sugihara, 2006, Hashimoto et al., 2009). In the present studies, none of the ethanol exposures produced any significant alteration of climbing fiber innervation within the Soma region. Previously, we identified alterations of climbing fiber innervation in the Molecular Layer region at PN14 that were mirrored by similar alterations in the Soma region (Pierce et al., 2010). We conclude, that the differences in climbing fiber development we have detailed, both at PN14 (Pierce et al., 2010) and in the present report at PN40, are not the result of a failure of climbing fiber translocation from the soma to the proximal dendritic tree structures.

A significant decrease in the Colocalized Volume Ratio (Fig. 4D) was identified for E7-9 ethanol exposure compared to controls (C7-9). The magnitude of this decrease was roughly 50% of the reduction produced by E4 or E4-6 (Fig. 4D). This suggests that the present findings are not dependent upon Purkinje cell loss but rather are concordant with that effect. However, the majority of Purkinje cell and climbing fiber alterations from ethanol exposure occurred during the PN4-6 time period.

In summary, we have shown for the first time that binge-like ethanol exposure during the rat cerebellar vulnerable period (PN4-6) for Purkinje cell development produces significant and permanent alterations of climbing fiber innervation of those Purkinje neurons that survive the well characterized ethanol-induced death. Thus, the damage from third-trimester equivalent ethanol exposure to the human fetus is likely to consist of more than just a reduced number of Purkinje neurons, but also includes altered functional connections of the cerebellar cortical circuit. Further studies to identify these alterations are underway.

4. Experimental procedures

4.1 Animal and tissue preparation

Timed-pregnant Sprague-Dawley rats (Harlan) delivered pups (designated PN0) in the University of Arkansas for Medical Sciences (UAMS) Division of Laboratory Animal Medicine. All animal care and experimental procedures were reviewed and approved by the Institutional Animal Care and Use Committee (IACUC) of UAMS prior to initiation of experimentation. Efforts to minimize the number of animals as well as to reduce any animal discomfort were included in this review. In addition, all experiments were carried out in accordance with the National Institutes of Health Guide for the Care and Use of Laboratory animals.

Rat pups of either sex were randomly assigned on PN4 to one of the experimental groups (see Table 1). Eight dams were utilized to produce 12 litters of rat pups. Each experimental group was comprised of pups from at least 3 (and in most cases 5–8) different litters (see Table 3). Ethanol exposure (E groups) was given at the dose of 4.5 g/kg body weight. Ethanol was administered one time a day, for one day on PN4 (E4 group), or for 3 days from PN4-6 (E4-6 group) or PN7-9 (E7-9 group). Intragastric intubation of a 15% (w/v) ethanol solution in Intralipid-II®, as previously described (Light et al., 2002), was utilized to deliver the daily ethanol dose. Isocaloric (vehicle) control pups (C groups) were treated in an identical manner, with the substitution of an isocaloric quantity of dextrose for the ethanol. Mother-reared controls (MRC) were not intubated. When performing the intubation process,

all pups (representing all groups) were removed together from the mother, weighed and kept in a warmed chamber. Pups were returned to the mother within 30–40 minutes.

PN40 was chosen for our analyses since by this time the final stage of climbing fiber innervation and maturation will have been established and the adult configuration attained. Three periods of Purkinje cell maturation have been identified (McKay and Turner, 2005). The early postnatal period (PN0 – PN9) is characterized primarily by the establishment of a monolayer configuration and the development of the cell soma and the beginnings of the dendritic structures. The period of rapid maturation (PN12 – PN18) is characterized by a significant expansion of the dendritic tree. The final stage (PN18 – PN90) has minor refinements of cell output and a plateau in growth of the dendritic area after PN30 (McKay and Turner, 2005). By PN40, the total dendritic length and area of the Purkinje neurons are nearly identical to that seen at PN90 (McKay and Turner, 2005).

On PN40, rats were weighed and then processed for the collection of the cerebellum to be analyzed by confocal microscopy. After an intraperitoneal injection of 50 mg/kg pentobarbital, intracardial perfusion with 0.05% heparin/0.9% NaCl was followed by 4% paraformaldehyde-lysine-periodate fixative (PLP), pH 7.4 (Pierce et al., 2006, Pierce et al., 2010). The cerebella were removed and post-fixed in PLP at 4°C overnight then cryoprotected with 30% sucrose in phosphate buffered saline (PBS), pH 7.4, and stored at 4°C. Mid-vermal sections (60 µm thick) were prepared by cryostat sectioning and stored free floating in 0.1M glycine/PBS with 0.02% Microcide. Additional mid-vermal sections of the same tissues were cut at 10 µm and collected on glass slides for cell counting.

Tissue was prepared for confocal imaging using immunofluorescence techniques. Purkinje cells, including their somas and dendritic structures, were selectively identified using monoclonal antibody to calbindin-D28k (CalB; 1:5,000, clone CB955, Sigma Chemical Co.) (Light et al., 2002, Pierce et al., 2010). Antibody to vesicular glutamate transporter 2 (VGluT2; 1:5,000, AB5907, Chemicon, Millipore Corp.) was used to visualize glutamate transporters within the climbing fibers (Hioki et al., 2003, Miyazaki et al., 2003, Takagishi et al., 2007, Pierce et al., 2010). Tissue was double-labeled with antibodies to CalB and VGluT2. Appropriate secondary antibodies (Alexa Fluor 594, Molecular Probes; Fluorescein conjugated affinity purified secondary, Millipore Corp.) were utilized to label Purkinje cells which were visible with fluorescence microscopy as red, and the climbing fibers as green.

4.2 Cell counting

Cell counts from lobule I were accomplished using mid-vermal sections that were cut at 10 µm. Tissue sections were prepared for cell counting using immunohistochemical techniques to visualize Purkinje cells. Monoclonal antibody to calbindin-D28k (CalB; 1:500, clone CB955, Sigma Chemical Co., St. Louis, MO) was used to selectively identify Purkinje cells, coupled with 3,3'-diaminobenzidine (DAB, Vector Laboratories) (Light et al., 2002, Pierce et al., 2010). Cell counting was done using a Zeiss Axioskop (Carl Zeiss, Thornwood, NY). One mid-vermal section of the cerebellum from each rat in the various groups was analyzed and all Purkinje cells in Lobule I were counted (Light et al., 2002). The purpose of cell counts was to confirm the presence of decreased Purkinje cells consistent with literature reports. In some cases we were not successful in obtaining useful sections of both 10 µm and 60 µm from the same cerebellum. Thus, there are different numbers of animals within the seven groups of PC counting compared to the confocal studies. The numbers for both the PC counting and the confocal analyses are presented in Table 1. There is no doubt that the stereological technique for cell counting provides greater precision in terms of the total number of cells within a defined region (Idrus et al., 2010). Nevertheless, we have previously demonstrated that counting one mid-vermal section provides identical data in

terms of the relative magnitude of cell loss and is an appropriate approach in the present study for confirming the well characterized cell loss (Pierce et al., 1999).

4.3 Blood ethanol concentrations

Blood ethanol concentrations (BEC) were determined from separate groups of pups. On PN4, pups were given a single ethanol dose, then analyzed 2.5 hours later. The animals were quickly decapitated and trunk blood was collected for analysis using head-space gas chromatography with flame-ionization detection per our established procedures (Ge et al., 2004).

4.4 Confocal imaging

Confocal image z-stacks were obtained from mid-sagittal slices of the lobule I region, most adjacent to lobule X. Lobule I was chosen because Purkinje cell loss in that lobule is greater than in any of the other lobules (Pierce et al., 1989, Bonthuis and West, 1990, Pierce et al., 1993). The sampling area was approximately 500×500 microns in each tissue. All tissues from each of the experimental and control groups were stained together as a cohort to ensure that the immunofluorescent staining was comparable across samples. In addition the confocal image acquisition was conducted so that all samples were imaged using consistent settings for laser power and detector gain.

The confocal images were collected from a Zeiss Pascal confocal microscope with a $20\times$ objective using the following parameters. Resolution was set at 512×512 pixels with 12 bit color. Multitrack settings were used with a 543 nm HeNe laser and a 488 nm argon laser. The optical slice was set at 2.0 microns with the slice thickness at 0.75 microns. This oversampling in the z-axis improved the resolution in that axis. Four scans were made per line with the mean of the signal recorded. The pinhole was set at 1 Airy unit.

4.5 Image analysis

One confocal image stack represented the data from one animal within a specific group. The confocal z-stacks were reconstructed into 3D image projections using the Imaris software (Bitplane AG, Zurich, Switzerland). The reconstructed images were first cropped so that only one layer of Purkinje cells was analyzed. Next, an isosurface was constructed for each fluorescent channel (calbindin-D28k and VGluT2) that provides the values for the total intensity of expression and the total volume that contains the expression (Hein et al., 2006, Marvizon et al., 2007). These isosurface constructions were divided into the Soma region and the molecular layer (MolLay) region for separate analysis.

4.6 Statistical analysis

Our hypothesis addresses specific questions that relate to treatment-timing combinations. As a result our first task was to identify whether the four control groups necessitated by these experiments were homogeneous across the different variables. To address this question we conducted a preliminary analysis of variance (ANOVA) including only the four control groups (MRC, C4, C4-6, and C7-9). This analysis served as a test of data consistency and to ensure the absence of control group differences.

Since there were no significant control group differences, the analysis for treatment-timing specific alterations involved a 2×3 factorial arrangement ANOVA. The six groups were: E4, E4-6, E7-9, C4, C4-6, and C7-9. Our approach consisted of first observing the interaction effect of E/C and timing. If this effect was significant at the 5% level, we directly observed the significance of the six custom contrasts (simple effects) of interest. The six custom contrasts of interest were: E4 vs C4, E4 vs E4-6, E4 vs E7-9, E4-6 vs C4-6, E4-6 vs E7-9; and E7-9 vs C7-9.

In the case of a non-significant interaction effect ($p > 0.05$) we observed the main effects, that is, the means of the E/C across timing, and the means of the timing, across E/C. In some situations, we included the significance of the six custom contrasts in order to provide additional insights.

We conducted the specific custom contrasts of interest using the mean-squared error values. Bonferroni multiple contrast methods were applied to control for type I error. All statistical analyses were conducted using SAS software (SAS Institute) and graphs were constructed using Prism (Graph Pad, Inc.) software.

Acknowledgments

This work was supported by NIH grant R03AA017300 to DRP, and a grant to DRP from the UAMS Medical Research Endowment fund for the Ed Harms Family Research Award. The Zeiss Pascal confocal microscope was located at the Scanning Electron Microscope/Confocal Facility at the University of Central Arkansas, Conway, AR, USA.

Abbreviations

PN	postnatal days
FASD	Fetal Alcohol Spectrum Disorder
MolLay	molecular layer of cerebellar cortex
Soma	soma layer of cerebellar cortex
VGLuT2	vesicular glutamate transporter 2
CalB	calbindin-D28k
BEC	blood ethanol concentration
PC	Purkinje cells

REFERENCES

- Altman, J.; Bayer, SA. Development of the cerebellar system : in relation to its evolution, structure, and functions. CRC Press; Boca Raton: 1997.
- Bonthius DJ, West JR. Alcohol-induced neuronal loss in developing rats: increased brain damage with binge exposure. *Alcohol Clin Exp Res.* 1990; 14:107–118. [PubMed: 1689970]
- Carta M, Mameli M, Valenzuela CF. Alcohol potently modulates climbing fiber-->Purkinje neuron synapses: role of metabotropic glutamate receptors. *J Neurosci.* 2006; 26:1906–1912. [PubMed: 16481422]
- Coffin JM, Baroody S, Schneider K, O'Neill J. Impaired cerebellar learning in children with prenatal alcohol exposure: a comparative study of eyeblink conditioning in children with ADHD and dyslexia. *Cortex.* 2005; 41:389–398. [PubMed: 15871603]
- Connor PD, Sampson PD, Streissguth AP, Bookstein FL, Barr HM. Effects of prenatal alcohol exposure on fine motor coordination and balance: A study of two adult samples. *Neuropsychologia.* 2006; 44:744–751. [PubMed: 16154165]
- Cudd TA. Animal model systems for the study of alcohol teratology. *Exp Biol Med (Maywood).* 2005; 230:389–393. [PubMed: 15956768]
- Dikranian K, Qin YQ, Labruyere J, Nemmers B, Olney JW. Ethanol-induced neuroapoptosis in the developing rodent cerebellum and related brain stem structures. *Brain Res Dev Brain Res.* 2005; 155:1–13.
- Dobbing, J. The later development of the brain and its vulnerability. In: Davis, JA.; Dobbing, J., editors. *Scientific Foundations of Paediatrics.* William Heinemann Medical Books; London: 1981. p. 744-759.

- Dobbing J, Sands J. Comparative aspects of the brain growth spurt. *Early Human Development*. 1979; 3:79–83. [PubMed: 118862]
- Fremeau RT Jr, Voglmaier S, Seal RP, Edwards RH. VGLUTs define subsets of excitatory neurons and suggest novel roles for glutamate. *Trends Neurosci*. 2004; 27:98–103. [PubMed: 15102489]
- Ge Y, Belcher SM, Pierce DR, Light KE. Altered expression of Bcl2, Bad and Bax mRNA occurs in the rat cerebellum within hours after ethanol exposure on postnatal day 4 but not on postnatal day 9. *Brain Res Mol Brain Res*. 2004; 129:124–134. [PubMed: 15469889]
- Goodlett CR, Lundahl KR. Temporal determinants of neonatal alcohol-induced cerebellar damage and motor performance deficits. *Pharmacol Biochem Behav*. 1996; 55:531–540. [PubMed: 8981583]
- Goodlett CR, Marcussen BL, West JR. A single day of alcohol exposure during the brain growth spurt induces brain weight restriction and cerebellar Purkinje cell loss. *Alcohol*. 1990; 7:107–114. [PubMed: 2328083]
- Goodlett CR, Peterson SD, Lundahl KR, Pearlman AD. Binge-like alcohol exposure of neonatal rats via intragastric intubation induces both Purkinje cell loss and cortical astrogliosis. *Alcohol Clin Exp Res*. 1997; 21:1010–1017. [PubMed: 9309310]
- Green JT. The effects of ethanol on the developing cerebellum and eyeblink classical conditioning. *Cerebellum*. 2004; 3:178–187. [PubMed: 15543808]
- Hamre KM, West JR. The effects of the timing of ethanol exposure during the brain growth spurt on the number of cerebellar Purkinje and granule cell nuclear profiles. *Alcohol Clin Exp Res*. 1993; 17:610–622. [PubMed: 8333592]
- Hashimoto K, Ichikawa R, Takechi H, Inoue Y, Aiba A, Sakimura K, Mishina M, Hashikawa T, Konnerth A, Watanabe M, Kano M. Roles of glutamate receptor delta 2 subunit (GluRdelta 2) and metabotropic glutamate receptor subtype 1 (mGluR1) in climbing fiber synapse elimination during postnatal cerebellar development. *J Neurosci*. 2001; 21:9701–9712. [PubMed: 11739579]
- Hashimoto K, Yoshida T, Sakimura K, Mishina M, Watanabe M, Kano M. Influence of parallel fiber-Purkinje cell synapse formation on postnatal development of climbing fiber-Purkinje cell synapses in the cerebellum. *Neuroscience*. 2009; 162:601–611. [PubMed: 19166909]
- Hein S, Kostin S, Schaper J. Adult rat cardiac myocytes in culture: 'Second-floor' cells and coculture experiments. *Exp Clin Cardiol*. 2006; 11:175–182. [PubMed: 18651028]
- Hioki H, Fujiyama F, Taki K, Tomioka R, Furuta T, Tamamaki N, Kaneko T. Differential distribution of vesicular glutamate transporters in the rat cerebellar cortex. *Neuroscience*. 2003; 117:1–6. [PubMed: 12605886]
- Ichise T, Kano M, Hashimoto K, Yanagihara D, Nakao K, Shigemoto R, Katsuki M, Aiba A. mGluR1 in cerebellar Purkinje cells essential for long-term depression, synapse elimination, and motor coordination. *Science*. 2000; 288:1832–1835. [PubMed: 10846166]
- Idrus NM, McGough NN, Riley EP, Thomas JD. Administration of Memantine During Ethanol Withdrawal in Neonatal Rats: Effects on Long-Term Ethanol-Induced Motor Incoordination and Cerebellar Purkinje Cell Loss. *Alcohol Clin Exp Res*. 2010
- Ito M. Cerebellar long-term depression: characterization, signal transduction, and functional roles. *Physiol Rev*. 2001; 81:1143–1195. [PubMed: 11427694]
- Kato Y, Takatsuki K, Kawahara S, Fukunaga S, Mori H, Mishina M, Kirino Y. N-methyl-D-aspartate receptors play important roles in acquisition and expression of the eyeblink conditioned response in glutamate receptor subunit delta2 mutant mice. *Neuroscience*. 2005; 135:1017–1023. [PubMed: 16165299]
- Kishimoto Y, Fujimichi R, Araishi K, Kawahara S, Kano M, Aiba A, Kirino Y. mGluR1 in cerebellar Purkinje cells is required for normal association of temporally contiguous stimuli in classical conditioning. *Eur J Neurosci*. 2002; 16:2416–2424. [PubMed: 12492436]
- Klintsova AY, Scamra C, Hoffman M, Napper RM, Goodlett CR, Greenough WT. Therapeutic effects of complex motor training on motor performance deficits induced by neonatal binge-like alcohol exposure in rats: II. A quantitative stereological study of synaptic plasticity in female rat cerebellum. *Brain Res*. 2002; 937:83–93. [PubMed: 12020866]
- Light KE, Belcher SR, Pierce DR. Time course and manner of Purkinje neuron death following a single ethanol exposure on postnatal day 4 in the developing rat. *Neuroscience*. 2002; 114:327–337. [PubMed: 12204202]

- Lopez-Bendito G, Shigemoto R, Lujan R, Juiz JM. Developmental changes in the localisation of the mGluR1alpha subtype of metabotropic glutamate receptors in Purkinje cells. *Neuroscience*. 2001; 105:413–429. [PubMed: 11672608]
- Marvizon JC, Perez OA, Song B, Chen W, Bunnett NW, Grady EF, Todd AJ. Calcitonin receptor-like receptor and receptor activity modifying protein 1 in the rat dorsal horn: localization in glutamatergic presynaptic terminals containing opioids and adrenergic alpha2C receptors. *Neuroscience*. 2007; 148:250–265. [PubMed: 17614212]
- Mason CA, Christakos S, Catalano SM. Early climbing fiber interactions with Purkinje cells in the postnatal mouse cerebellum. *J Comp Neurol*. 1990; 297:77–90. [PubMed: 1695909]
- McKay BE, Turner RW. Physiological and morphological development of the rat cerebellar Purkinje cell. *J Physiol*. 2005; 567:829–850. [PubMed: 16002452]
- Meyer LS, Kotch LE, Riley EP. Neonatal ethanol exposure: functional alterations associated with cerebellar growth retardation. *Neurotoxicol Teratol*. 1990; 12:15–22. [PubMed: 2314357]
- Miyazaki T, Fukaya M, Shimizu H, Watanabe M. Subtype switching of vesicular glutamate transporters at parallel fibre-Purkinje cell synapses in developing mouse cerebellum. *Eur J Neurosci*. 2003; 17:2563–2572. [PubMed: 12823463]
- Napper RM, West JR. Permanent neuronal cell loss in the inferior olive of adult rats exposed to alcohol during the brain growth spurt: a stereological investigation. *Alcohol Clin Exp Res*. 1995; 19:1321–1326. [PubMed: 8561309]
- Nassimi M, Schleh C, Lauenstein HD, Hussein R, Lubbers K, Pohlmann G, Switalla S, Sewald K, Muller M, Krug N, Muller-Goymann CC, Braun A. Low cytotoxicity of solid lipid nanoparticles in in vitro and ex vivo lung models. *Inhal Toxicol*. 2009; 21:104–109. [PubMed: 19558241]
- NSDUH. The NSDUH Report: Substance Use among Women During Pregnancy and Following Childbirth. Substance Abuse and Mental Health Services Administration, O. o. A. S; Rockville, M: 2009.
- Pierce DR, Cook CC, Hinson JA, Light KE. Are oxidative mechanisms primary in ethanol induced Purkinje neuron death of the neonatal rat? *Neurosci Lett*. 2006; 400:130–134. [PubMed: 16516384]
- Pierce DR, Goodlett CR, West JR. Differential neuronal loss following early postnatal alcohol exposure. *Teratology*. 1989; 40:113–126. [PubMed: 2772847]
- Pierce DR, Hayar A, Williams DK, Light KE. Developmental alterations in olivary climbing fiber distribution following postnatal ethanol exposure in the rat. *Neuroscience*. 2010; 169:1438–1448. [PubMed: 20542091]
- Pierce DR, Serbus DC, Light KE. Intra-gastric intubation of alcohol during postnatal development of rats results in selective cell loss in the cerebellum. *Alcohol Clin Exp Res*. 1993; 17:1275–1280. [PubMed: 8116842]
- Pierce DR, Williams DK, Light KE. Purkinje cell vulnerability to developmental ethanol exposure in the rat cerebellum. *Alcohol Clin Exp Res*. 1999; 23:1650–1659. [PubMed: 10549998]
- Riley EP, McGee CL. Fetal alcohol spectrum disorders: an overview with emphasis on changes in brain and behavior. *Exp Biol Med (Maywood)*. 2005; 230:357–365. [PubMed: 15956765]
- Roebuck TM, Simmons RW, Mattson SN, Riley EP. Prenatal exposure to alcohol affects the ability to maintain postural balance. *Alcohol Clin Exp Res*. 1998; 22:252–258. [PubMed: 9514315]
- Sotelo C. Cellular and genetic regulation of the development of the cerebellar system. *Prog Neurobiol*. 2004; 72:295–339. [PubMed: 15157725]
- Strata P, Rossi F. Plasticity of the olivocerebellar pathway. *Trends Neurosci*. 1998; 21:407–413. [PubMed: 9735949]
- Streissguth AP, Barr HM, Martin DC, Herman CS. Effects of maternal alcohol, nicotine, and caffeine use during pregnancy on infant mental and motor development at eight months. *Alcohol Clin Exp Res*. 1980; 4:152–164. [PubMed: 6990818]
- Sugihara I. Microzonal projection and climbing fiber remodeling in single olivocerebellar axons of newborn rats at postnatal days 4–7. *J Comp Neurol*. 2005; 487:93–106. [PubMed: 15861456]
- Sugihara I. Organization and remodeling of the olivocerebellar climbing fiber projection. *Cerebellum*. 2006; 5:15–22. [PubMed: 16527759]

- Takagishi Y, Hashimoto K, Kayahara T, Watanabe M, Otsuka H, Mizoguchi A, Kano M, Murata Y. Diminished climbing fiber innervation of Purkinje cells in the cerebellum of myosin Va mutant mice and rats. *Dev Neurobiol.* 2007; 67:909–923. [PubMed: 17506494]
- Thomas JD, Goodlett CR, West JR. Alcohol-induced Purkinje cell loss depends on developmental timing of alcohol exposure and correlates with motor performance. *Brain Res Dev Brain Res.* 1998; 105:159–166.
- Thomas JD, Wasserman EA, West JR, Goodlett CR. Behavioral deficits induced by binge-like exposure to alcohol in neonatal rats: importance of developmental timing and number of episodes. *Dev Psychobiol.* 1996; 29:433–452. [PubMed: 8809494]
- Ventura SJ, Abma JC, Mosher WD, Henshaw SK. Estimated pregnancy rates by outcome for the United States, 1990-2004. *Natl Vital Stat Rep.* 2008; 56:1–25. 28. [PubMed: 18578105]
- Watanabe M. Molecular mechanisms governing competitive synaptic wiring in cerebellar Purkinje cells. *Tohoku J Exp Med.* 2008; 214:175–190. [PubMed: 18323688]

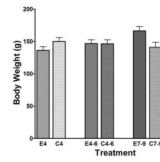


Figure 1.

Body weights of PN40 rats following ethanol exposure at 4.5 g/kg during the early postnatal period. Analyses did not identify any significant control group differences ($F_{(3,20)}=0.35$, $p > 0.05$). There was a significant interaction ($F_{(2,29)}=4.3$; $p<0.05$); however, custom contrasts ($p<0.05$) did not verify any significant differences. C4, C4-6, C7-9 = Isocaloric vehicle control groups; E4, E4-6, E7-9 = Ethanol exposure groups; (see Table 1). Error bars represent SEM; $MRC40 = 150.65 \pm 5.88$.

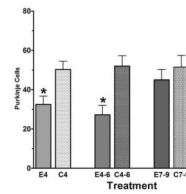


Figure 2.

Purkinje cell (PC) numbers in Lobule I of PN40 rats following ethanol exposure at 4.5 g/kg during the early postnatal period. No significant control group differences ($F_{(3,22)}=0.18$, $p > 0.05$) were identified. There was no significant interaction ($F_{(2,30)} = 1.5$; $p > 0.05$) and no significant main effect of timing ($F_{(2,30)} = 1.5$; $p > 0.05$); however a significant main effect of treatment ($F_{(1,30)}=16.3$; $p<0.01$) was identified. Custom contrasts at the $p<0.05$ level identified significant differences for E4 vs C4 (*) and E4-6 vs C4-6(*). Error bars represent SEM; MRC40 = 47.6 ± 4.2 .

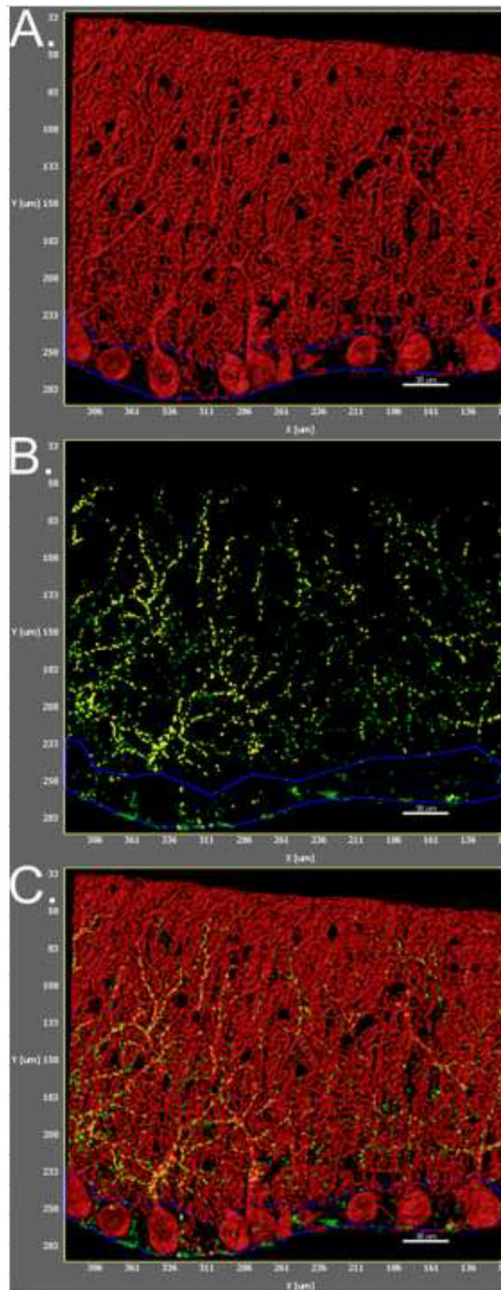


Figure 3.

Rendered images of Lobule I Purkinje cells with VGlut2/climbing fiber innervation. Images were produced using Imaris software. **A.** Rendered image of the calbindin-D28k (CalB) immunostaining demonstrating cerebellar Purkinje cells. Note that the soma layer is outlined in blue. The scale bar in each image is 30 microns. **B.** Rendered image of the VGlut2 immunostaining. This represents the VGlut2 positive portion of the climbing fibers from the inferior olive. The VGlut2 immunostaining is represented as green puncta and the specific VGlut2 immunostaining that is co-localized with CalB is represented as yellow puncta. **C.** Combined red and green channels showing the interactions of the Purkinje cells with the climbing fibers.

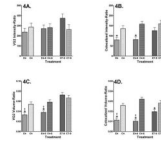


Figure 4.

Alterations in Climbing Fiber endings in the Molecular Layer of Lobule I on PN40 following ethanol exposure at 4.5 g/kg during the early postnatal period. MRC40 = mother reared control group; C4, C4-6, C7-9 = Isocaloric vehicle control groups; E4, E4-6, E7-9 = Ethanol exposure groups; (see Table 1). Error bars represent SEM.

A. VGlut2 expression intensity relative to total PC tissue volume (VG2 Intensity-Ratio).

There were no significant control group differences ($F_{(3, 20)}=0.05$; $p > 0.05$) that impact the conclusions. There was no significant interaction ($F_{(2,29)} < 1$) and no significant main effect of treatment ($F_{(1,29)} < 1$) or timing ($F_{(2,29)} < 1$). MRC40 = 275.81 ± 35.14 .

B. Co-localized expression intensity relative to total PC tissue volume (Co-localized Intensity-Ratio). There were no significant control group differences ($F_{(3, 20)}=0.46$; $p > 0.05$) that impact the conclusions. A significant interaction ($F_{(2, 29)}=5.1$; $p<0.02$) was observed. Custom contrasts at the $p<0.05$ level identified significant differences for E4 vs C4 (*) and for E4-6 vs C4 -6(*). MRC40 = 148.88 ± 13.39 .

C. VGlut2 expression volume relative to total PC tissue volume (VG2 Volume-Ratio).

There were no significant control group differences ($F_{(3, 20)}=0.72$; $p > 0.05$) that impact the conclusions. There was no significant interaction ($F_{(2, 29)} = 1.1$; $p>0.05$) observed. A significant main effect of treatment ($F_{(1,29)} = 22.9$; $p<0.01$) and no significant main effect of timing ($F_{(2, 29)} = 2.8$; $p>0.05$) was observed. Custom contrasts at the $p<0.05$ level identified significant differences only for E4 vs C4 (*), E4 vs E7-9 (†), E4-6 vs C4-6 (*), and E4-6 vs E7-9 (†). MRC40 = 0.06 ± 0.005 .

D. Co-localized expression volume relative to total PC tissue volume (Co-localized Volume-Ratio). There were no significant control group differences ($F_{(3, 20)}=1.46$; $p > 0.05$) that impact the conclusions. A significant interaction ($F_{(2, 29)} = 5.1$; $p<0.02$) was observed. Custom contrasts at the $p<0.05$ level identified significant differences for E4 vs C4 (*), E4 vs E7-9 (†); E4-6 vs C4-6 (*), E4-6 vs E7-9 (†); and E7-9 vs C7-9 (*). MRC40 = 0.03 ± 0.002 .

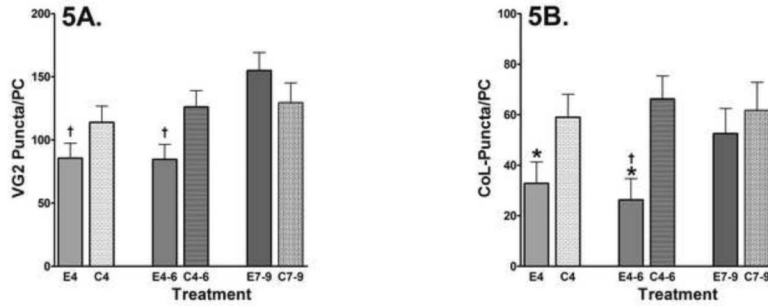


Figure 5.

Alterations in the number of puncta representing Climbing Fiber endings in the Molecular Layer region of Lobule I on PN40 following ethanol exposure at 4.5 g/kg during the early postnatal period. MRC40 = mother reared control group; C4, C4-6, C7-9 = Isocaloric vehicle control groups; E4, E4-6, E7-9 = Ethanol exposure groups; (see Table 1). Error bars represent SEM.

A. Total VGlut2 puncta present in the molecular layer region expressed on a per Purkinje cell basis. (VG2 Puncta/PC). There were no significant control group differences ($F_{(3,20)}=0.37$; $p > 0.05$) that impact the conclusions. No significant interaction ($F_{(2, 29)} = 3.2$; $p>0.05$) and no significant main effect of treatment ($F_{(1,29)} = 1.9$; $p>0.05$) was identified. However a significant main effect of timing ($F_{(2, 29)} = 5.4$; $p<0.02$) was observed. Custom contrasts at the $p<0.05$ level identified significant differences only for E4 vs E7-9 (†) and E4-6 vs E7-9 (†). MRC40 = 112.05 ± 12.0 .

B. Total co-localized puncta present in the molecular layer region expressed on a per Purkinje cell basis. (CoL-Puncta/PC). There were no significant control group differences ($F_{(3, 20)}=0.17$; $p > 0.05$) that impact the conclusions. A significant interaction ($F_{(2, 29)} = 3.7$; $p<0.05$) was observed. Custom contrasts at the $p<0.05$ level identified significant differences for E4 vs C4 (*), E4-6 vs C4-6 (*), and E4-6 vs E7-9 (†). MRC40 = 56.27 ± 9.48 .

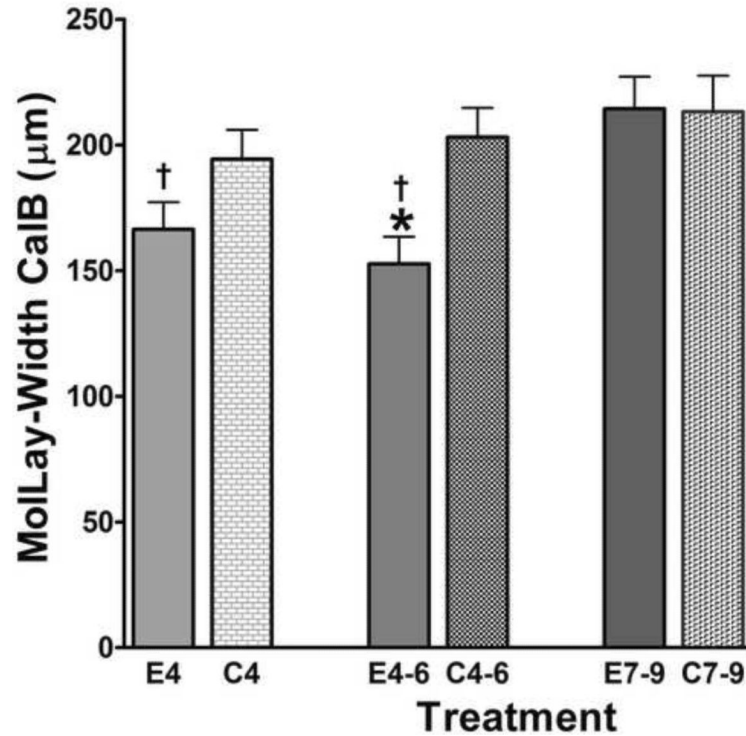


Figure 6.

Alterations in MolLay-Width of the CalB staining of Lobule I on PN40 following ethanol exposure at 4.5 g/kg during the early postnatal period. MRC40 = mother reared control group; C4, C4-6, C7-9 = Isoleucine vehicle control groups; E4, E4-6, E7-9 = Ethanol exposure groups; (see Table 1). Error bars represent SEM. There were no significant control group differences that impact the data ($F_{(3,20)}=0.38$, $p > 0.05$). No significant interaction ($F_{(2, 29)}=2.2$; $p > 0.05$) was observed. Significant main effects of treatment ($F_{(1,29)} = 6.9$; $p < 0.02$) and timing ($F_{(2, 29)} = 4.9$; $p < 0.02$) were identified. Custom contrasts at the $p < 0.05$ level identified significant differences for E4 vs E7-9 (†), E4-6 vs C4-6 (*), and E4-6 vs E7-9 (†). MRC40 = 199.40 ± 10.00 .

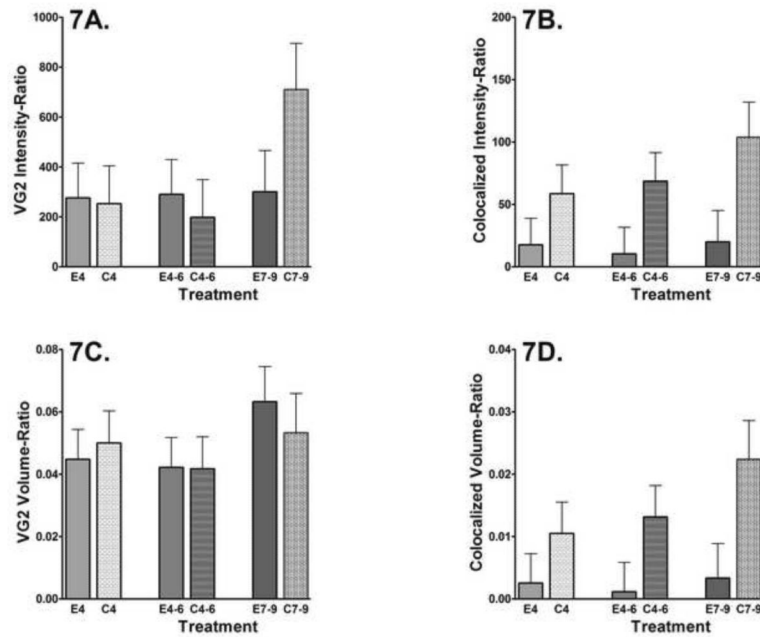


Figure 7.

Alterations in Climbing Fiber endings in the Soma region of Lobule I on PN40 following ethanol exposure at 4.5 g/kg during the early postnatal period. MRC40 = mother reared control group; C4, C4-6, C7-9 = Isocaloric vehicle control groups; E4, E4-6, E7-9 = Ethanol exposure groups; (see Table 1). Error bars represent SEM.

A. VGlut2 expression intensity relative to total PC tissue volume (VG2 Intensity-Ratio).

There were no significant control group differences ($F_{(3, 20)}=1.30$; $p > 0.05$) that impact the conclusions. MRC40 = 264.68 ± 155.05 . There was no significant interaction ($F_{(2,29)}=1.3$; $p>0.05$) and no significant main effect of treatment ($F_{(1,29)} < 1$) or timing ($F_{(2,29)} = 1.5$; $p>0.05$).

B. Alterations in the Co-localized expression intensity relative to total PC tissue volume

(Co-localized Intensity-Ratio). There were no significant control group differences ($F_{(3, 20)}=0.27$; $p > 0.05$) that impact the conclusions. There was no significant interaction ($F_{(2,29)} < 1$) and no significant main effect of treatment ($F_{(1,29)} < 1$) or timing ($F_{(2,29)} = 1.1$; $p>0.05$). MRC40 = 74.05 ± 28.2 .

C. Alterations in the VGlut2 expression volume relative to total PC tissue volume (VG2

Volume-Ratio). There were no significant control group differences ($F_{(3, 20)}=0.41$; $p > 0.05$) that impact the conclusions. No significant interaction ($F_{(2, 29)} < 1$) and no significant main effect of treatment ($F_{(1,29)} < 1$) or timing ($F_{(2, 29)} < 1$) were present. MRC40 = 0.06 ± 0.01 .

D. Alterations in relative Co-localized expression volume relative to total PC tissue volume

(Co-localized Volume-Ratio). There were no significant control group differences ($F_{(3, 20)}=0.39$; $p > 0.05$) that impact the conclusions. No significant interaction ($F_{(2, 29)} < 1$) was observed. A significant main effect of treatment ($F_{(1,29)} = 9.4$; $p<0.01$) with no significant main effect of timing ($F_{(2, 29)} < 1$) was present. MRC40 = 0.02 ± 0.006 .

Table 1

Experimental groups definitions and the number of animals represented.

Group	Description	Confocal Imaging	Cell Counting
E4	Ethanol exposed PN4 only	7	8
E4-6	Ethanol exposed PN4-6	7	6
E7-9	Ethanol exposed PN7-9	5	5
C4	Isocaloric control PN4	6	8
C4-6	Isocaloric control PN4-6	6	5
C7-9	Isocaloric control PN7-9	4	4
MRC	Mother reared control	8	9

Table 2

Definition of image analysis end-points

VGluT2 Intensity Ratio	VGluT2 intensity/calbindin-D28k volume
VGluT2 Volume Ratio	VGluT2 channel volume/calbindin-D28k volume
Co-localized Intensity Ratio	Co-localized intensity/calbindin-D28k volume
Co-localized Volume Ratio	Co-localized channel volume/calbindin-D28k volume
VGluT2 Puncta/PC	VGluT2 puncta/Purkinje cell
CoL-Puncta/PC	Co-localized puncta/Purkinje cell
MolLay-Width	Radial distance from Soma/MolLay border to pial surface

Table 3

Number of litters represented within the experimental groups (PC counting).

	E4	E4-6	E7-9	C4	C4-6	C7-9	MRC
4.5 g/kg	7 (5)	7 (6)	5 (5)	3 (5)	6 (5)	4 (4)	8 (9)